

Deep Space One Investigations of Ion Propulsion Plasma Interactions: Overview and Initial Results

J. Wang, D. Brinza, R. Goldstein, J. Polk, M. Henry

Jet Propulsion Laboratory, California Institute of Technology, Pasadena, CA 91109

D.T. Young, J.J. Hanley

Southwest Research Institute, San Antonio, TX 78228

J. Nordholt, D. Lawrence, M. Shappirio

Los Alamos National Laboratory, Los Alamos, NM 87545

1. Introduction

The launch of NASA's **New Millennium** Deep Space One (DS1) mission on October 24, 1998 marks the beginning of interplanetary science missions using spacecraft operated on **solar electric propulsion**. The DS1 spacecraft, propelled by a 30cm **Xenon ion thruster**, is currently on a trajectory for a July 29, 1999 encounter with asteroid 1992 KD and possible 2001 encounters with comets Wilson-Harrington and Borrelly. As the New Millennium DS1 is a **technology validation** mission, a primary objective of DS1 is to flight validate solar electric propulsion for interplanetary science missions, including the characterization of ion propulsion induced interactions and their effects on spacecraft payloads, subsystems, and **solar wind measurements**.

In ion thrusters, propellant ions are accelerated electrostatically by a system of grids to form a high velocity beam (typically with an energy of about 1 KeV). Electrons are emitted from a neutralizer for neutralization of the ion beam. The propellant that remains un-ionized also flows out of the thruster exit at a thermal speed corresponding to the thruster wall temperature (~ 500 K). Charge-exchange collisions will occur between the fast moving propellant ions and the slow moving neutrals which generate slow moving ions and fast moving neutrals. Hence, for a spacecraft operated on ion thruster there is a continued presence of a plasma plume composed by propellant ions, neutralizing electrons, un-ionized neutral propellant, and a low energy charge-exchange plasma generated within the plume. As the ion thruster plume may lead to a variety of complex plasma interactions, such as plume backflow contamination, plume interactions with space-

craft, and plume interactions with the solar wind, both science and engineering concerns have long been raised over the potential effects from ion thruster operation.

Ion thrusters have never been flown on an interplanetary spacecraft. Although ion thruster induced interaction has been a subject of extensive experimental and theoretical studies (for example, see *Jones et al.*[1970], *Carruth*[1981]; *Samanta Roy et al.*[1996a,b], *Wang et al.*[1996], *Katz et al.*[1997], and references therein), there have been no comprehensive in-flight investigations due to lack of flight opportunities. While in-flight investigations have been attempted on SERT II spacecraft in low Earth orbit for a mercury ion thruster and on ATS 6 spacecraft in geosynchronous orbit for a cesium ion thruster, almost all existing experimental data on ion thruster plume are obtained from ground tests of ion thrusters, with the majority of the data obtained for mercury and cesium ion thrusters [*Carruth*, 1981; *Jones et al.*, 1970]. As it is impossible to create in a vacuum tank a plasma environment similar to that under typical solar wind conditions, it is difficult to quantitatively predict ion propulsion induced plasma interactions for an interplanetary spacecraft based on ground test data.

The DS1 mission provides the first ever comprehensive in-flight investigations of ion propulsion induced interactions and their effects. This paper presents an overview of the investigation on ion propulsion plasma interactions. This investigation is being carried out by investigators from Jet Propulsion Lab (JPL), Southwest Research Institute (SwRI), and Los Alamos National Lab (LANL) under both DS1 mission science investigations and the NASA Solar electric propulsion Technology Application Readiness (NSTAR) program. This

paper also reports an initial analysis of the first ever in situ measurements of ion propulsion induced plasma environment for an interplanetary spacecraft.

2. DS1 Investigations of Ion Propulsion Plasma Interactions: an Overview

In this section we present a brief overview of the investigations of ion propulsion plasma interactions from DS1. The investigations include in situ measurements, correlated data analysis, modeling, and comparison of modeling results with data.

NSTAR Ion Thruster

The ion thruster used on DS1 is developed under the NSTAR program. The 30 cm xenon NSTAR thruster has an input power range of 600 to 2500 W. At full thrust level, the propellant Xe^+ ions are accelerated to form a beam with an energy of about 1100 eV (exit beam velocity of $v_b \simeq 3.5 \times 10^6$ cm/s). and a beam current of about 1.8 A. Under typical operating conditions at full thrust level, the average beam ion density outside the thruster exit is about $n_{b0} \sim 10^9$ cm $^{-3}$. The propellant ions form a divergent beam with a divergence half angle about 15 to 20° due to the curvature of the thruster exit surface. This beam is kept quasi-neutral by electrons emitted from the neutralizer. The propellant that remains un-ionized flows out of the thruster exit in free molecular flow with a thermal speed corresponding to the thruster wall temperature of ~ 500 K. The density of the neutral plume near the thruster exit is typically about $n_{n0} \sim 10^{12}$ cm $^{-3}$ and remains quasi-steady due to the low charge-exchange collision rate. A detailed description of the in-flight validation of the NSTAR ion thruster is presented in [Polk *et al.*, 1999].

Instrumentation

DS1 carries two science instrument packages: the Miniature Integrated Camera and Spectrometer (MICAS) and the Plasma Experiment for Planetary Exploration (PEPÉ), and one ion propulsion diagnosis package: the Ion propulsion Diagnostic Subsystem (IDS). Ion propulsion related investigations are based on IDS and PEPÉ measurements. IDS is located at about 1 meter away from the ion thruster exit. PEPÉ is located on the upper spacecraft surface at the opposite end of DS1 from the thruster.

IDS

The Ion Propulsion Diagnostic Subsystem (P.I.: D. Brinza, JPL), shown in Fig.1, is a part of the NSTAR ion propulsion system and is dedicated to characterize ion thruster induced environment and contamination.

IDS has several components, including two quartz crystal microbalances, two calorimeters, a retarding potential analyzer (RPA), a planar Langmuir probe (LP), a spherical Langmuir probe, two flux gate magnetometer, a search coil magnetometer, and a plasma wave antenna.

This paper will analyze data obtained from the RPA (IDS-RPA) and the planar Langmuir probe (IDS-LP1). IDS-RPA has a voltage range of 0 to +100 Vdc and a current range of 0 to 100 μ A). The opening to the RPA is 20 cm 2 . IDS-LP1 has a voltage range of -12 to +12 Vdc and a current range of -0.5 to +40 mA. The current collecting area of IDS-LP1 is 50 cm 2 .

PEPE

The Plasma Experiment for Planetary Exploration (P.I.: D. Young, SwRI), shown in Fig.2, is a novel state-of-the-art plasma sensor developed by SwRI and LANL. The main objectives of PEPÉ are to study solar wind plasma physics, cometary plasma processes, and asteroid environments, and contribute to the evaluation of ion thruster induced environment. PEPÉ simultaneously measures the differential flux of electrons and mass-resolved ions over a solid angle range of 2.8π sr and an energy/charge range of 8 eV/q to 32,000 eV/q. Mass/charge is resolved using a unique time-of-flight system with a mass range of 500 amu/q and resolution $M/\delta M = 30$. PEPÉ's sensitivity is approximately 10^{-2} cm 2 sr eV/eV for electrons and 10^{-3} cm 2 sr eV/eV for ions. PEPÉ has an elevation angle range from -45° to $+45^\circ$ and an azimuthal angle of the full 360° range (minus spacecraft obstructions). The observed solid angle is resolved into 256 angular pixels of $5^\circ \times 22.5^\circ$ for electrons and varying pixel sizes of $5^\circ \times 5^\circ$ up to $5^\circ \times 45^\circ$ for ions. Electrostatic deflection optics are employed to scan the PEPÉ field-of-view (FOV) by $\pm 45^\circ$ in elevation angle once every 0.51 s. PEPÉ obtains a full 3-dimensional scan in about 64 seconds. PEPÉ data are analyzed by casting the detector counting rates in the form of 3-dimensional velocity distribution functions in phase space.

Investigations

Ion thruster can generate a complex set of plasma interactions. In the near-field region of the spacecraft, it is well known that the low energy charge-exchange ions can be pushed out of the plume by local electrostatic potential and backflow to interact with the spacecraft. As the plume potential is influenced by the density difference between the plume center and the ambient plasma, the charge-exchange ion interactions may differ significantly in different ambient plasmas [Wang *et al.*, 1995]. For DS1, the plume-spacecraft interaction is further complicated by the 100 volt SCARLET solar array which may influence spacecraft charging as well as

interact with DS1's plasma environment. In addition, the presence of the solar wind may induce plume-solar wind interactions. In the vicinity of the thruster, since the thruster plume will dominate the spacecraft environment due to its much higher density, the plume may modify the solar wind as it flows past the plume region. Far away from the thruster where the plume density has decreased to a level that the solar wind plasma and fields can penetrate the plume, the plume ions may couple with the solar wind through collective plasma effects [Wang *et al.*, 1999]. The DS1 investigations will address all these issues by analyzing data from correlated PEPE and IDS measurement and computer particle simulation modeling.

Both IDS and PEPE have made extensive plasma measurements during ion thruster operations. These observations will provide the following information: velocity distributions of the xenon ions, solar wind protons, and electrons; charge-exchange ion energy and flux; electron temperature; plume potential; the magnetic field; and both low frequency plasma waves and high frequency plasma waves. These measurements are currently being analyzed.

Since IDS and PEPE make only single point measurements, modeling based on multi-dimensional computer particle simulations is also necessary to provide a more complete description of the physics. A set of particle-in-cell (PIC) based simulation models have been developed to assist the data analysis and interpretation. A 3-D full particle electrostatic PIC code will be used to simulate near-thruster plasma interactions, study the electron characteristics, derive an effective electron temperature, and study the underlying factors that controls the plume potential. A 3-D hybrid electrostatic PIC with Monte-Carlo collision code will be used to simulate near-spacecraft plasma interactions and obtain the distributions of electric field and charge-exchange ions around the spacecraft as a function of solar wind parameters and thruster levels. A 3-D hybrid electromagnetic PIC code will be used to simulate global scale plume-solar wind interactions, with the emphasis on the physics of solar wind flowing around the plume, and study possible plume modifications of the solar wind properties. A 2-D hybrid electromagnetic PIC code will be used to investigate potential local plume ion-solar wind couplings via electromagnetic plasma instabilities.

3. Characterization of Ion Thruster Induced Plasma Environment: Initial Results

In this section, we present an initial characterization of ion propulsion induced plasma environment for DS1

based on IDS-RPA, IDS-LP1, and PEPE measurements obtained during a DS1 activity called S-Peak.

DS1 S-Peak (Jan. 22, 1999)

The DS1 S-Peak activity occurred on Jan 22nd, 1999. S-Peak is designed to determine peak power point for the SCARLET arrays. During this time period, the ion thruster operated at low, medium, and high thrust levels with high Xe flow. Both the IDS and PEPE were operating before, during, and after the S-Peak activity.

Fig.3 shows several thruster parameters obtained from flight data, including beam current and voltage, propellant efficiency, and flow rates. Thrusting started at around 9:36pm. The thruster operation stepped through three thrust levels, Th0, Th4, and Th12. Thrusting stopped at about 10:16pm. The specific impulse for these three thrust levels are ~ 2000 , ~ 2900 , and ~ 3200 for Th0, Th4, and Th12 respectively. Due to the short S-Peak time, the thruster operating condition did not reach an equilibrium state. Averaged key thruster performance parameters are listed in Table 1.

To benchmark the induced plasma environment at different thrust levels, we estimate the average charge exchange ion production rate at thruster exit from these thruster parameters. The average charge exchange ion production rate at thruster exit is given by

$$\frac{dn_{cex0}}{dt} = n_{b0}n_{n0}v_b\sigma_{cex}$$

where $n_{b0} = I_b/ev_bA$ is the average beam ion density at thruster exit, n_{n0} the average neutral density at thruster exit, v_b the beam ion velocity, and σ_{cex} the charge-exchange ion collision cross section.

n_{n0} can be calculated from the measured main flow rate, cathode flow rate, and the discharge propellant efficiency η_d , and by assuming that the un-ionized propellant exits through the grids in free-molecular flow with a temperature close to that of the thruster discharge chamber walls T_w :

$$n_{n0} = \frac{\dot{N}}{A_n \sqrt{8kT_w/\pi m_{Xe}}}$$

where \dot{N} is the number of Xe particles per second, and is converted from the discharge charge chamber flow rate, $\dot{m}_d = (1 - \eta_d)(\dot{m}_m + \dot{m}_c)$. A_n is the flow-through area through the grids and is about 0.24 of the thruster exit area for the NSTAR thruster. σ_{cex} can be estimated from curve fitting of the measured collision cross section for $Xe^+ - Xe$ charge-exchange [Rapp, 1962; Samanata Roy *et al.* 1996a]:

$$\sigma_{cex} = (k_1 \ln v_b + k_2)^2 \times 10^{-20} \text{ m}^2$$

where v_b is beam ion velocity with unit in m/s, $k_1 = -0.8821$, and $k_2 = 15.1262$. For the three thrust level considered here, σ_{cex} ranges from $3.65 \times 10^{-15} \text{ (cm}^2\text{)}$ for Th0 to $3.37 \times 10^{-15} \text{ (cm}^2\text{)}$ for Th12. The calculated beam plasma density, neutral density, and the charge-exchange ion production rate near thruster exit are listed in Table 2. Note that all the parameters listed in Table 2 are averaged estimations at each thrust level because the thruster did not have time to reach its equilibrium condition during S-Peak.

Charge-Exchange Plasma Measured by IDS

Figs. 4 through 6 show the data obtained from IDS-RPA and IDS-LP1 during S-Peak. Fig.4 shows the time history of the IDS-RPA sweep. The time period, labeled by spacecraft clock, is from about 9:35pm to about 10:07pm, i.e., from before the start of ion thruster through part of the Th12. Fig.5 shows the averaged IDS-RPA sweep curve at each thrust level. Fig.6 shows the averaged IDS-LP1 sweep curve at each thrust level.

As shown in Fig.4, the IDS-RPA starts to collect an ion current as soon as the ion thruster starts firing. The sudden change in the saturated ion current corresponds to the change in thrust level. The voltages measured by the RPA and LP are all relative to the spacecraft ground. From Fig.5, we can obtain the saturated ion current and ion energy relative to the spacecraft potential averaged for each thrust level. From Fig.6, we can obtain the local plasma potential relative to the spacecraft potential, and the electron temperature averaged for each thrust level. Table 3 lists these results.

The observations show that the saturated ion current collected by IDS-RPA increased from $\sim 2.2 \mu\text{A}$ to $\sim 2.4 \mu\text{A}$ when the thrust level changed from Th0 to Th4 and decreased to $\sim 1.75 \mu\text{A}$ when the thrust level changed from Th4 to Th12. The average energy (relative to spacecraft ground) of the ions collected ranges from 14 eV (at Th0 and Th4) to 19 eV (at Th12). The local plasma potential (relative to spacecraft ground) at IDS location is from 6 Volts (at Th0) to 4 Volts (at Th12). The local electron temperature is about 1 to 2 eV.

Since IDS is located about 1 meter away from the ion thruster and is well outside of the primary plume region, the ions measured by IDS-RPA is from the charge-exchange ions transported outward from the primary plume. We next derive the charge-exchange ion environment from these IDS results. We denote Φ_p , Φ_{IDS} , Φ_{scg} to be the average electrostatic potential inside the thruster plume, the potential at the location of IDS, and the potential of the spacecraft ground, respectively. As the charge-exchange ions originate from the very cold neutrals (temperature 0.04eV), the ion energy measured

by RPA represents the difference between the electric potential inside the plume (where these charge-exchange ions are produced) and the spacecraft ground potential, $\Phi_p - \Phi_{scg}$. From the charge-exchange ion energy measured by IDS-RPA and the local plasma potential measured by IDS-LP, we find the difference between the plume potential and the local plasma potential

$$\Phi_p - \Phi_{IDS} = (\Phi_p - \Phi_{scg}) - (\Phi_{IDS} - \Phi_{scg})$$

Hence, the average energy of the charge exchange Xe^+ ions collected by IDS is $E_{cex} = e(\Phi_p - \Phi_{IDS})$, which gives the average Xe^+ ion velocity at the IDS location

$$v_{cex} = \sqrt{\frac{2e(\Phi_p - \Phi_{IDS})}{m_{Xe}}}$$

From the charge-exchange ion current density measured by RPA, one finds the charge-exchange ion density at the IDS location:

$$n_{cex} = \frac{J_{cex}}{ev_{cex}}$$

The results of the charge-exchange ion plasma environment are listed in Table 4.

We find that the current density associated with charge exchange ion outflow is about 10^{-7} A/cm^2 and the charge exchange ion density at the IDS location is about 10^6 cm^{-3} . Not surprisingly, the differences between the charge-exchange ion densities at each thrust level correlates to the changes in the charge-exchange ion production rate estimated in the previous section. When thrust level changed from Th0 to Th4, an increase in the beam ion current drove up d_{cex}/dt , and hence IDS-RPA observed an increase in charge-exchange ion collection. When thrust level changed from Th4 to Th12, even though the beam ion current increased, a more significant decrease in the neutral density due to high η_d drove down the d_{cex}/dt , and hence IDS-RPA observed a decrease in charge-exchange ion collection.

The observations show that the plume potential increases significantly as beam current increases. This is because the plasma potential decreases as a high density plasma expands into a more dilute plasma (under the mesothermal process). Hence, the potential difference between the plume center and the ambient plasma is controlled by the density difference between the beam ions and the ambient plasma. The observations also show that there is an increase in electron temperature as beam current increases. This is probably because that the electrons emitted from the neutralizer undergo a stronger acceleration and heating from the more strong electrostatic field associated with high plume potential.

It is interesting to observe that, while the plume potential $\Phi_p - \Phi_{IDS}$ differs by 60% between the low and high thrust levels, the ratio of the plume potential to the electron temperature is relatively a constant at about $(\Phi_p - \Phi_{IDS})/T_e \sim 7$.

Charge-Exchange Plasma Measured by PEPE

PEPE is located on the opposite side of DS1 from the ion thruster to minimize the effects from ion thruster operation. However, during ion thruster operation, PEPE also measured significant Xe^+ ions. In the data reported here DS1 is oriented so that the PEPE field of view scans above and below the plane of the ecliptic. In the orthogonal direction PEPE views 360° instantaneously. During the period of interest here, PEPE covered a complete energy-angle scan once every 65.5s.

Because of the PEPE energy cutoff at 8 eV for both ions and electrons, it is not possible to make an accurate estimate of the spacecraft chassis potential when, as appears to be the case here, it is below the cutoff.

Fig.7 is a color spectrogram showing ion counts measured by PEPE as function of time for a time period containing S-Peak on Jan 22 of 1999. The spectrogram covers a time period from 21:00 through 24:00. The top panel displays ion energy per charge in eV/e, the middle panel shows the measured ion distribution in elevation angle, and the bottom panel shows the distribution in azimuth angle. The color scale on the right gives the count level logarithmically.

The band of high count level just above 1000 eV is from the solar wind protons. What is notable, however, is the high count rate beginning at about 22:00 at about 15-35 eV, corresponding to the period in which IPS was operating at the Th12 level (See Table 1). The elevation and azimuth panels show that these ions reach PEPE from the direction of the thruster beam. Spectrogram showing the time of flight (TOF) mass spectrum response of PEPE also showed a broad count rate peak during this period which corresponds in mass/charge to Xe^+ . Hence, these are apparently the low energy charge exchange Xe^+ ions. We note that the energy of Xe^+ measured by PEPE corresponds to that measured by IDS during Th12.

Fig.8 is a similar color spectrogram, but for the electrons measured by PEPE. The lower limit of electron energy sweep was normally set at 8eV. As shown in the time period of 22:30 to 24:00, when the thruster is off. The low energy high count rate seen here is due largely to the photoelectron cloud surrounding the spacecraft. This is a normal occurrence in sunlight. There is also another high count rate at about 40 eV. This second high count rate is still being investigated. One possi-

ble explanation is that this is due to the effects of the SCARLET solar array. The solar array has a potential difference of 100 Volts. The negative end of the solar array is grounded at the spacecraft. The wiring of the solar array is such that the solar array has an exposed edge of +50 volts above spacecraft potential. Hence, the solar array could accelerate some of the solar wind electrons near the spacecraft to about +50 eV above spacecraft potential.

In the time period prior to 22:30, the lower limit in electron energy sweep was increased to about 15 eV to avoid a possible overload of the detector, since very high count rates had been measured during previous ion thruster operation. Coincident with the low energy ion Count rate increase in Fig.7, the electron count rate also increases above background during Th12. This indicates that ion thruster operation also produces a low energy electron cloud around DS1 denser than that of photoelectrons. This is apparently caused by the electrons that drift along with the outflow charge-exchange ions to keep the charge-exchange plasma quasi-neutral.

Thus PEPE has conclusively shown the presence of low energy (20 eV) charge exchange Xe^+ ions flowing back to the spacecraft during Th12, although the flux is orders of magnitude lower than that of the solar wind.

Fig.8 also shows that there is a cut-off of high energy electrons coincident with the entire ion thruster operating period. The reason for the cut-off could be that ion thruster operation changed the spacecraft potential. It could also be because the ion beam and charge-exchange ions significantly changed the sheath structure surrounding the spacecraft for solar wind electron collection. The exact cause of this cut-off, however, is still not clear.

Discussions

Recently, several computer particle simulation models are developed for ion thruster charge-exchange plasma [Samanata Roy, 1996a,b; Wang et al., 1996; Katz et al., 1997; Gardner et al., 1997]. For instance, Wang et al. [1996] developed a 3-dimensional electrostatic PIC code coupled with a Monte Carlo collision calculation for charge-exchange ion generation for the DS1 ion thruster plume. They predicted that, under typical thruster operating conditions, the outflow of charge-exchange Xe^+ should lead to Xe^+ density of $10^6 cm^{-3}$ and Xe^+ ion current density of $10^{-7} A/cm^2$ at about 1 meter away from the thruster. Similar results were also obtained by Katz et al. [1997] and Gardner et al. [1997] using a 2-dimensional axis-symmetric finite element particle code. The IDS measurements appear to be in good agreement with these preflight predictions.

A detailed analysis of PEPE collection of Xe^+ ions requires one first obtain the electric field in the vicinity of DS1 and then trace the trajectories of the Xe^+ ions from their origin in the thruster plume to PEPE's field of view. Such a calculation requires information on the distribution of spacecraft charging potential on DS1 surface. Due to lack of such information, previous simulations [Wang *et al.*, 1996; Gardner *et al.*, 1997; Katz *et al.*, 1997] have not studied the detailed effects of spacecraft potential on Xe^+ surrounding DS1.

The fact that PEPE observes substantial charge-exchange Xe^+ ions only during Th12, when the charge-exchange ion current measured by IDS-RPA and the charge-exchange ion production rate are significantly lower than that for the other two thrust levels, suggests that the dominant factor underlying charge-exchange ion backflow is the electric potential distribution surrounding spacecraft rather than charge-exchange ion production. This is not surprising. The Debye length under typical solar wind conditions is on the order of 10 meters. Hence, except for the small area surrounding the thruster, DS1 is covered by a "thick" sheath whose thickness is much larger than the spacecraft dimension. Therefore, once a charge-exchange ion is pushed out of the plume by the electric field within the plume, it will fall into the potential field of spacecraft sheath, and its orbit will be similar to that of charged particles near an electrostatic prob in the orbital motion limited (OML) regime [Chung *et al.*, 1979].

For a qualitative discussion, we consider the spacecraft to be a spherical probe with a radius r_{sc} and a surface potential Φ_{sc} . We describe the particle orbits in a spherical coordinate centered in the probe. Let us consider that a charge-exchange ion is generated at location "0" within the plume and subsequently pushed out from the plume at location "1" on the plume edge. Location 1 has a distance L from the spacecraft surface along the thrust direction. Let us take the potential difference between the plume center and the plume edge to be $\Delta\Phi_p$. This Xe^+ leaves the plume with a total energy $E_1 = e\Phi_p$, a velocity $v_{1\theta} = \sqrt{2e\Delta\Phi_p/m}$, and an angular momentum with respect to spacecraft center

$$\Omega_1 = m(L + r_{sc})v_{1\theta} = m(L + r_{sc})\sqrt{2e\Delta\Phi_p/m}$$

In the OML regime, the invariants of motion are the angular momentum and the total energy. Hence, once outside the plume, this Xe^+ 's orbit is determined by

$$\frac{1}{2}mv_r^2 + \frac{\Omega_1^2}{2mr^2} + e\Phi = E_1$$

If this Xe^+ is to be collected by PEPE at the opposite

side of spacecraft surface, we must have

$$E_1 - \left(\frac{\Omega_1^2}{2mr_{sc}^2} + e\Phi_{sc}\right) \geq 0$$

This leads to

$$1 + \frac{L}{r_{sc}} \leq \sqrt{\frac{\Phi_p - \Phi_{sc}}{\Delta\Phi_p}}$$

Hence, the necessary condition for charge-exchange ions originated from the thruster plume to backflow to the opposite side of spacecraft is that the potential difference between the plume and the spacecraft must be sufficiently large :

$$\Phi_p - \Phi_{sc} > \Delta\Phi_p$$

$\Delta\Phi_p$ is mainly determined by the density difference between the beam center and the beam edge, which in turn is controlled by beam divergence. Hence, the critical factor will be the potential difference between the plume and the spacecraft, $\Phi_p - \Phi_{sc}$. The IDS-RPA shows that $\Phi_p - \Phi_{sc}$ during Th12 is about 30% higher than that during Th0 and Th4. This may explain why PEPE measures Xe^+ only during Th12 but not during Th0 and Th4.

5. Summary and Conclusions

For the first time, a comprehensive in-flight investigation of ion propulsion plasma interaction is being carried out on an interplanetary spacecraft, and in situ measurements of the ion propulsion induced plasma environment surrounding an interplanetary spacecraft has been obtained in the solar wind. Initial analysis of IDS and PEPE measurements obtained during a particular DS1 activity, S-Peak, revealed interesting correlations between the induced plasma environment and thruster operating conditions. At the IDS location which is about 1 meter away from the ion thruster, IDS measured a charge-exchange Xe^+ ion current density of $\sim 10^{-7} A/cm^2$ and a charge-exchange ion density of $\sim 10^6 cm^{-3}$ during ion thruster firings. These measurements appear to be in good agreement with pre-flight predictions based on computer particle simulations. The measured Xe^+ ion density near thruster exit is 5 to 6 orders magnitude larger than the solar wind plasma density. The quantitative differences in the measured Xe^+ density at different thrust levels correlates with the charge-exchange ion production rate estimated from thruster data. IDS measurements also show that the plume potential will increase significantly as the beam current increases. This suggests that the main underlying physical process that controls the global plume

potential is the expansion of the high density propellant plasma. Hence, the plume potential sensitively depends on the density difference between the beam ions and the ambient plasmas.

While IDS measured more charge-exchange ions during the two lower thrust levels, PEPE, which is on the opposite side of the ion thruster, observed significant Xe^+ ions only at the highest thrust level. This suggests that the dominant factor underlying charge-exchange ion backflow is the electric potential distribution surrounding spacecraft rather than charge-exchange ion production. A simple analysis shows that, in order for charge-exchange ions to backflow to the front side of an interplanetary spacecraft, the spacecraft potential needs to be sufficiently negative with respect to the plume. For DS1, it appears that charge-exchange ion backflow can occur only at high thrust levels.

Acknowledgments

We acknowledge the contributions from the entire PEPE team and IDS team as well as technical support provided by the DS1 mission and the NSTAR project. We acknowledge many helpful discussions with P.C. Liewer (JPL), B. Goldstein (JPL), S.P. Gary (LANL), and I. Katz (Maxwell Labs). The work at Jet Propulsion Laboratory, California Institute of Technology was performed under a contract with NASA, and was supported by the NASA New Millennium Deep Space 1 mission and the NASA Solar Electric Propulsion Technology Application Readiness Project. The work at Southwest Research Institute was supported by NASA DS1 mission. The work at Los Alamos National Laboratory was supported by NASA contracts WO-9066, WO-9165, and WO-9138 in the building of PEPE as well as support for data validation, display, distribution, and analysis.

References

Gardner, B., et al., Predictions of NSTAR charge-exchange ions and contamination backflow, *IEPC Pap.* 97-043, 1997.

Carruth, M., Ed., Experimental and analytical evaluation of ion thruster/spacecraft interactions, *JPL Publication* 80-92, 1981.

Chung, P., L. Talbot, and K. Touryan, *Electric Probes in Stationary and Flowing Plasmas*, Springer-Verlag, 1979.

Jones, S., J. Staskus, and D. Byers, Preliminary results of SERT II spacecraft potential measurements, *NASA TM X-2083*, 1970.

Katz, I., V. Davis, J. Wang, and D. Brinza, Electrical potentials in the NSTAR charge-exchange plume, *IEPC Pap.* 97-042, 1997.

Polk, J., et al., In-flight validation of the NSTAR ion thruster technology on the Deep Space One mission, *AIAA Pap.* 99-2274, 1999.

Rapp, D. and W. Francis, Charge-exchange between gaseous ions and atoms, *J. Chemical Phys.*, 37(11), 1962, pp2631.

Samanta Roy, R., D. Hastings, and N. Gatsonis, Ion-thruster modeling for backflow contamination, *J. Spacecraft Rockets*, 33(4), 1996a, pp525.

Samanta Roy, R., D. Hastings, and N. Gatsonis, Numerical study of spacecraft contamination and interactions by ion-thruster effluents, *J. Spacecraft Rockets*, 33(4), 1996b, pp535.

Wang, J. and J. Brophy, "3D Monte-Carlo particle-in-cell simulations of ion thruster plumes", *AIAA Pap.* 95-2826, 1995.

Wang, J., J. Brophy, and D. Brinza, 3-D simulations of NSTAR ion thruster plasma environment, *AIAA Pap.* 96-3202, 1996.

Wang, J., S.P. Gary, and P.C. Liewer, "Electromagnetic heavy ion/proton instabilities", submitted to *J. Geophys. Res.*, 1999.

Table 1: S-Peak Thrust Conditions, Jan 22nd, 1999

Thrust Level	I_b (A)	E_b (eV)	η_d
Th0 (6)	.52	649	.32
Th4 (36)	.82	1003	.52
Th12 (83)	1.40	1095	.88

Table 2: Parameters at Thruster Exit for S-Peak

Thrust Level	J_{b0} (A/m^2)	V_{b0} (km/s)	n_{b0} ($1/cm^3$)	\dot{N}_{n0} (1/s)	n_{n0} ($1/cm^3$)	dn_{cex0}/dt ($1/cm^3s$)
Th0 (6)	7.36	29.8	1.54×10^9	6.2×10^{18}	1.4×10^{12}	2.3×10^{13}
Th4 (36)	11.6	37.0	1.96×10^9	4.3×10^{18}	0.95×10^{12}	2.4×10^{13}
Th12(83)	19.8	38.7	3.22×10^9	1.1×10^{18}	0.23×10^{12}	1.0×10^{13}

Table 3: IDS Results

Thrust Level	I (μA)	E_{cex} (eV)	T_e (eV)	$\Phi_{IDS} - \Phi_{scg}$ (V)
Th0 (6)	2.2	15	1.17	6
Th4 (36)	2.4	14	1.33	5
Th12 (83)	1.75	19	2.09	4

Table 4: Induced Plasma Environment at IDS

Thrust Level	$\Phi_p - \Phi_{IDS}$ (V)	$(\Phi_p - \Phi_{IDS})/T_e$	J_{cex} (A/cm^2)	v_{cex} (km/s)	n_{cex} (cm^{-3})
Th0 (6)	9	7.7	1.1×10^{-7}	3.45	2×10^6
Th4 (36)	9	6.8	1.2×10^{-7}	3.45	2.2×10^6
Th12(83)	15	7.18	0.87×10^{-7}	4.46	1.2×10^6

Figure Captions

Figure 1: The Ion Propulsion Diagnostic Subsystem (IDS).

Figure 2: The Plasma Experiment for Planetary Exploration (PEPÉ).

Figure 3: Thruster parameters obtained from DS1 flight data for S-Peak, Jan 22, 1999.

Figure 4: Time history of IDS-RPA sweep for S-Peak. Time shown is from about 9:35pm to 10:06pm.

Figure 5: IDS-RPA sweep curve averaged for each thrust level.

Figure 6: IDS-LP1 sweep curve averaged for each thrust level.

Figure 7: Spectrogram for single ions measured by PEPÉ. Top panel: ion energy per charge in eV/e. Middle panel: ion distribution in elevation angle. Bottom panel: ion distribution in azimuth angle.

Figure 8: Spectrogram for electrons measured by PEPÉ. Top panel: electron energy. Middle panel: electron distribution in elevation angle. Bottom panel: electron distribution in azimuth angle.

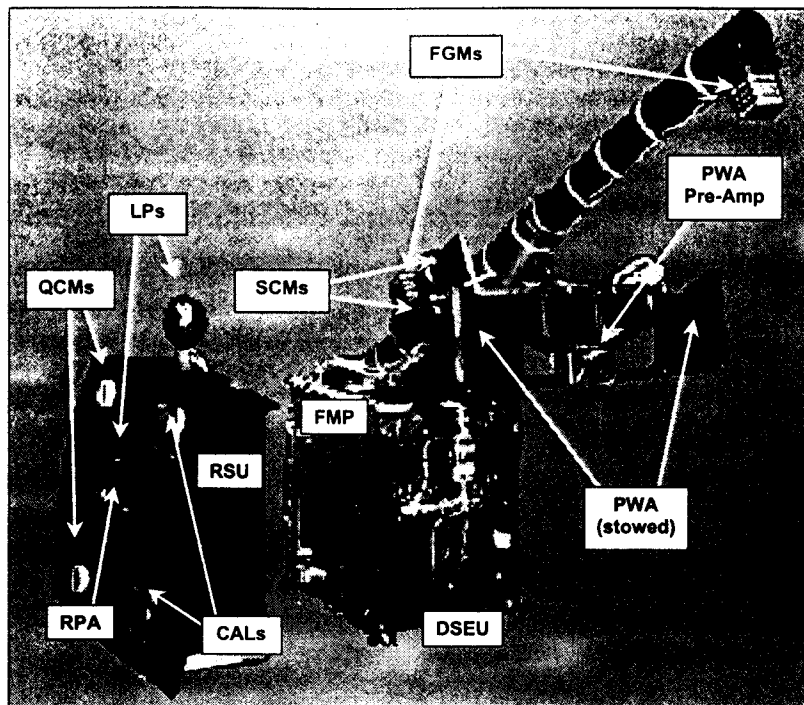


Figure 1

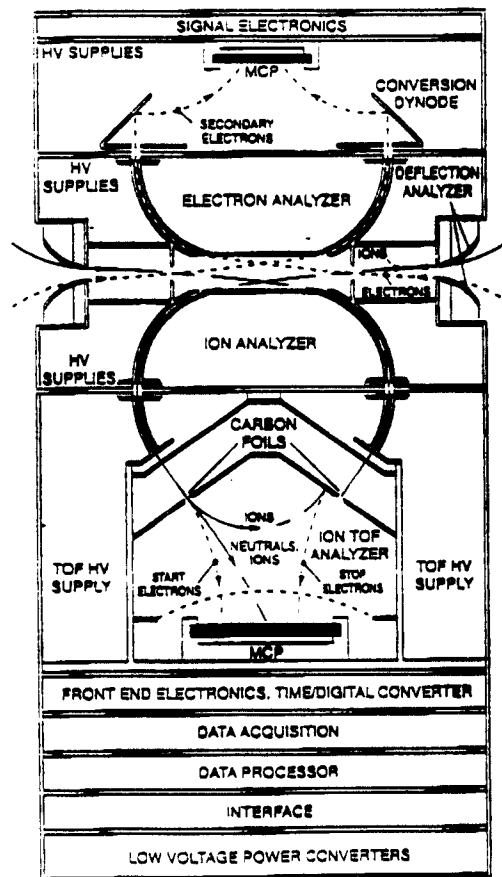


Figure 2

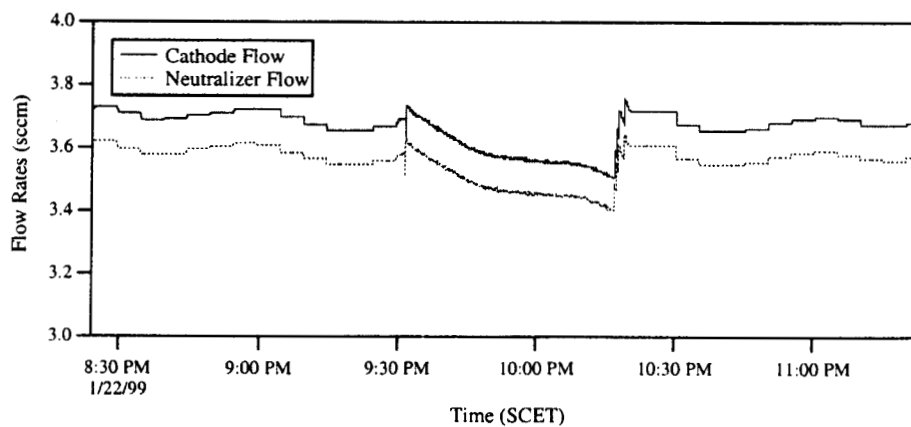
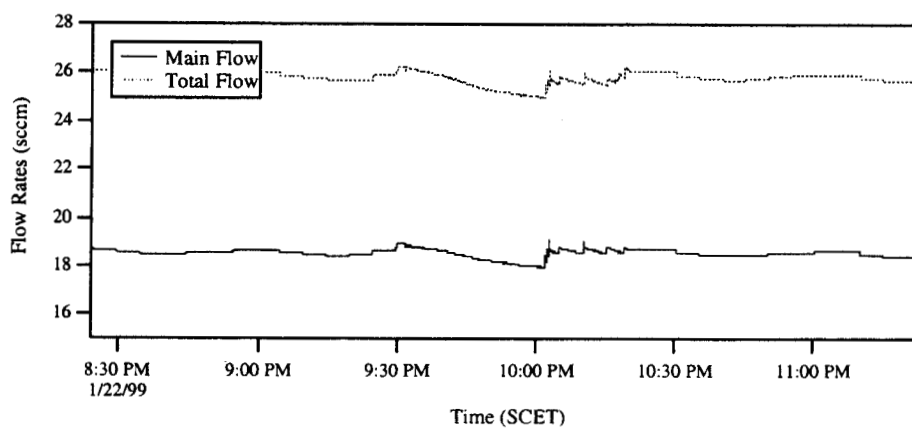
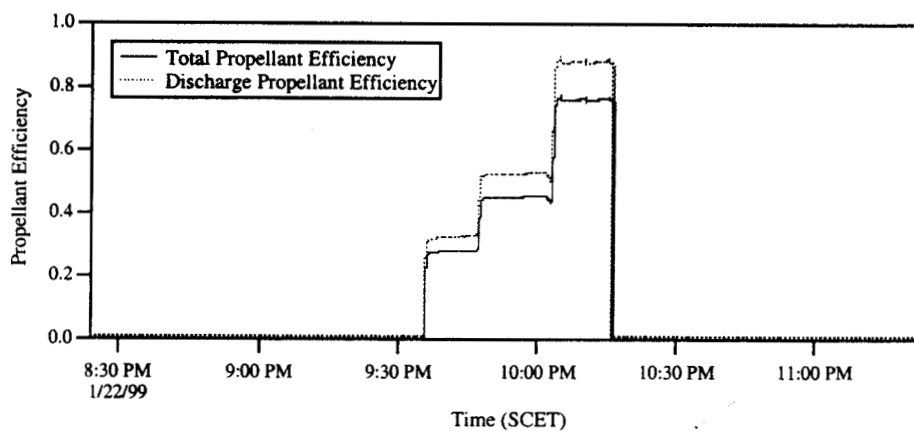
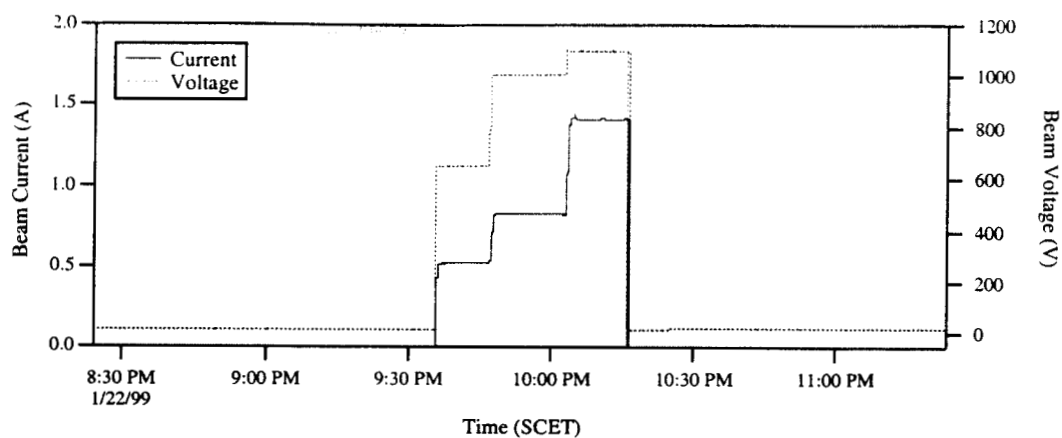


Figure 3

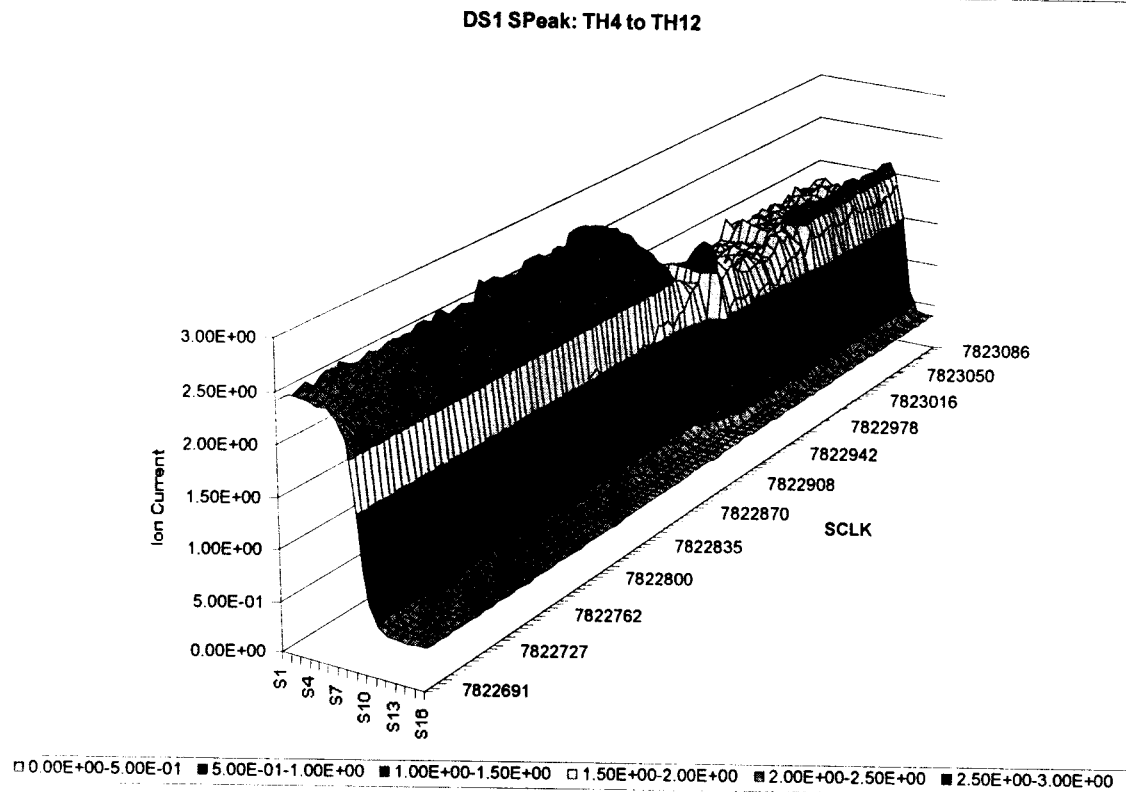
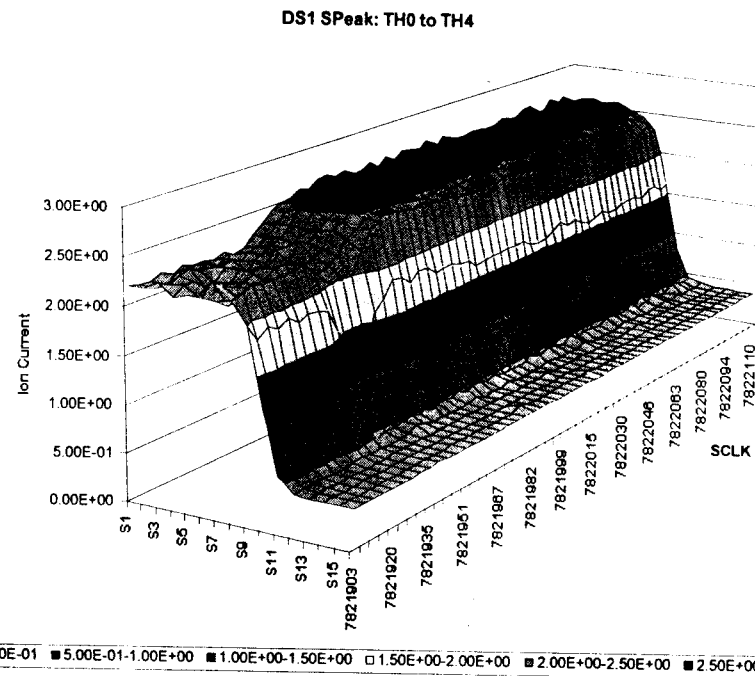
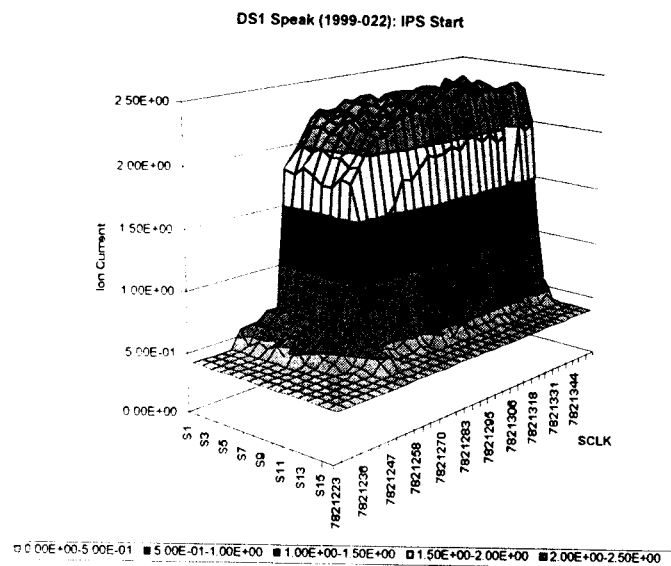


Figure 4

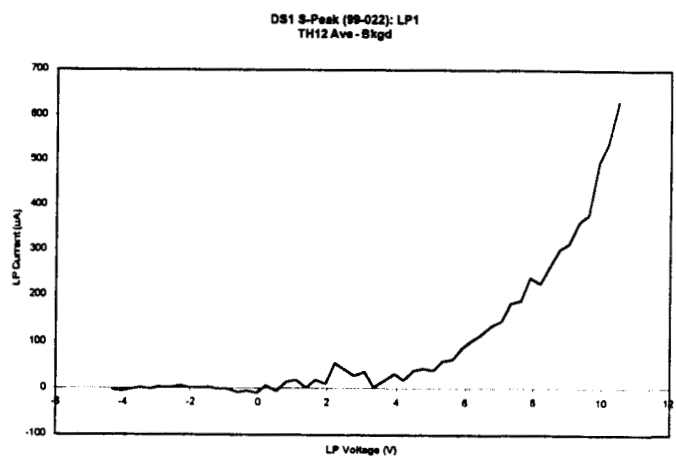
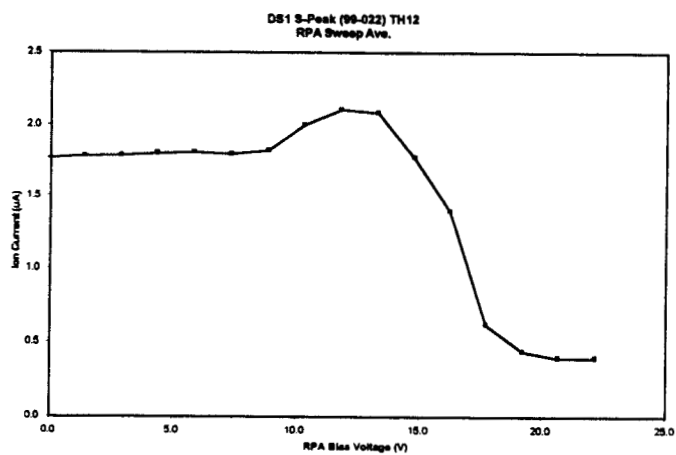
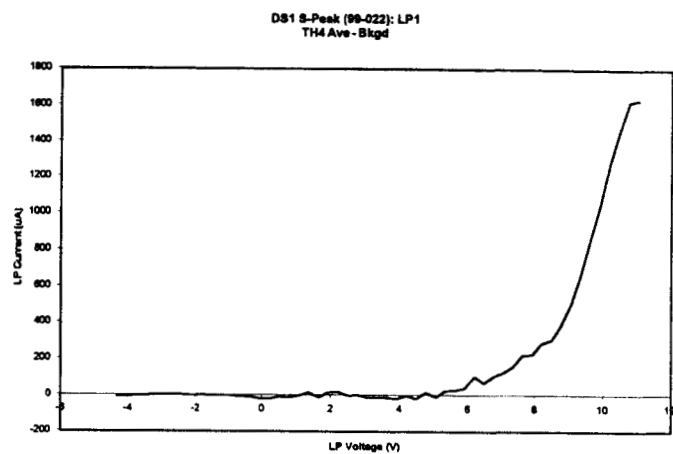
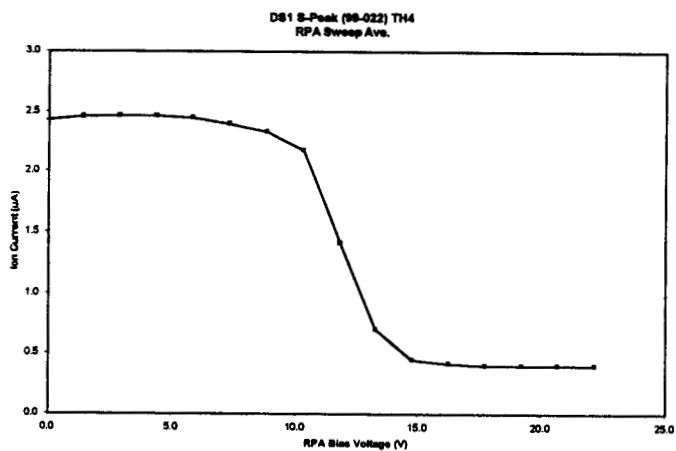
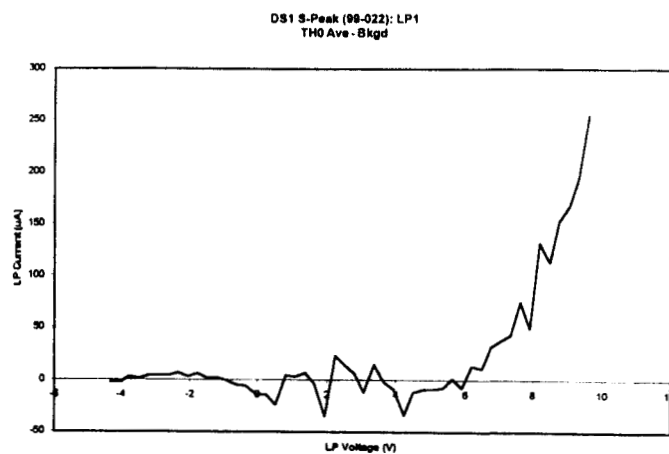
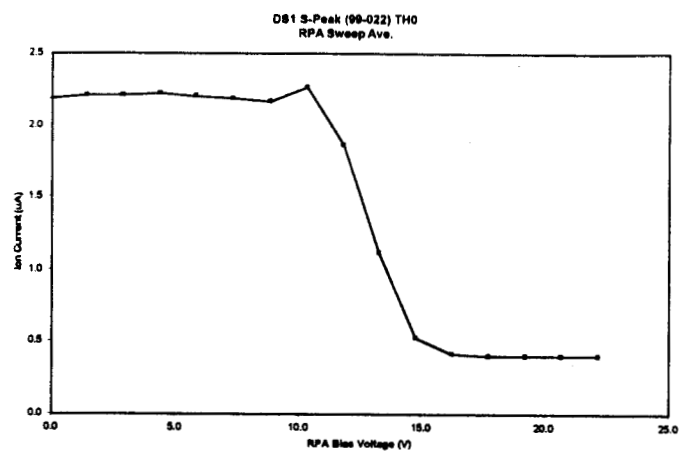


Figure 5

Figure 6

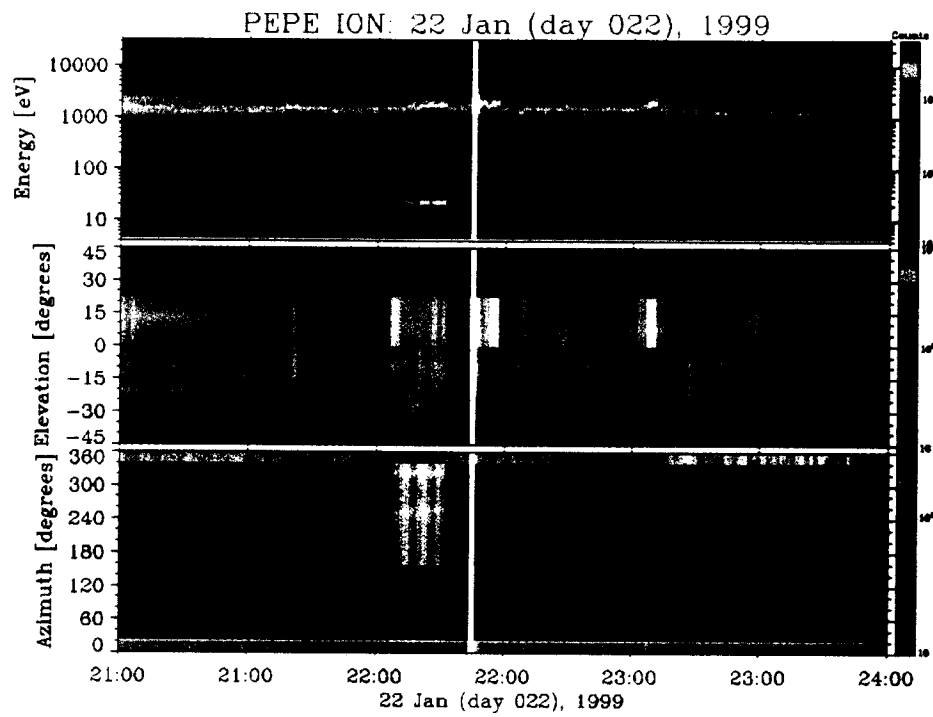


Figure 7

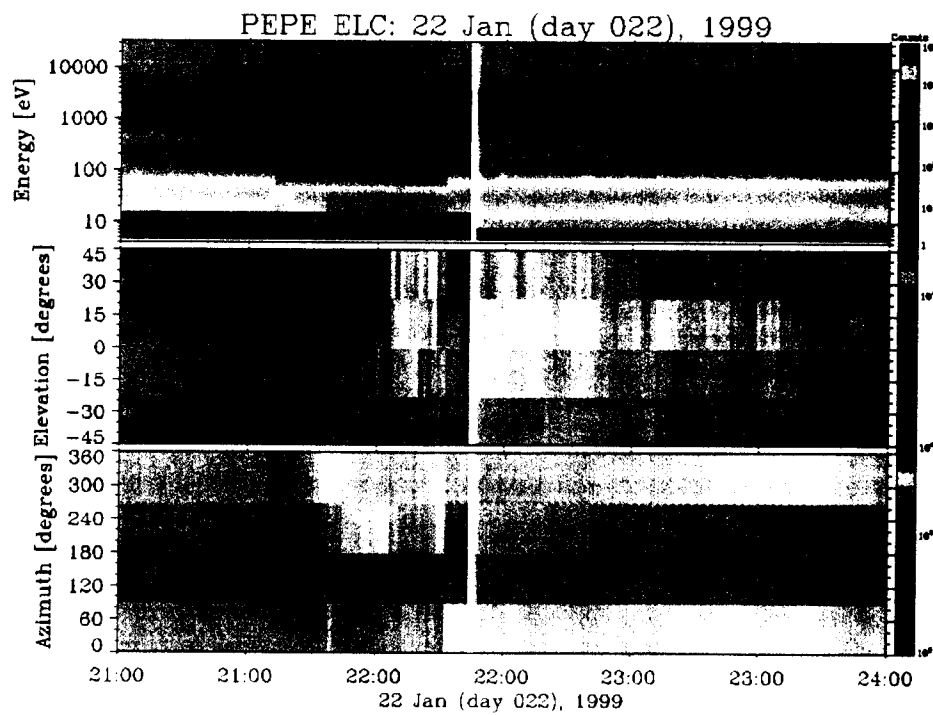


Figure 8